



12 March 1999

**CHEMICAL
PHYSICS
LETTERS**

Chemical Physics Letters 302 (1999) 113–118

Spectroscopic characterization of the $\text{Zn}(4s^2) \cdot \text{Ne}[^1\Sigma^+]$ and $\text{Zn}(4s4p\pi) \cdot \text{Ne}[^1\Pi_1]$ van der Waals states

John G. McCaffrey¹, D. Bellert, Allen W.K. Leung, W.H. Breckenridge*

Department of Chemistry, University of Utah, Salt Lake City, UT 84112, USA

Received 20 November 1998; in final form 21 December 1998

Abstract

The $\text{Zn}(4s^2) \cdot \text{Ne}[^1\Sigma^+]$ and the $\text{Zn}(4s4p\pi) \cdot \text{Ne}[^1\Pi_1]$ states have been characterized by laser-induced fluorescence spectroscopy. Bond lengths were determined from simulations of the partially-resolved rotational structure of the $^1\Pi \leftarrow ^1\Sigma^+$ transitions, while bond strengths were estimated from a Birge–Sponer extrapolation with allowance for consistent errors resulting from similar procedures in the analogous $\text{Cd} \cdot \text{Ne}$ and $\text{Hg} \cdot \text{Ne}$ transitions. The van der Waals bonding in these states is discussed briefly and compared to that in the analogous $\text{M} \cdot \text{RG}$ states, where $\text{M} = \text{Mg}, \text{Zn}, \text{Cd}, \text{Hg}$ and $\text{RG} = \text{Ne}, \text{Ar}, \text{Kr}, \text{Xe}$. © 1999 Elsevier Science B.V. All rights reserved.

1. Introduction

Transitions from the $\text{M}(ns^2) \cdot \text{RG}[^1\Sigma^+]$ ground-state van der Waals complexes to their more strongly-bound $\text{M}(nsnp\pi) \cdot \text{RG}[^1\Pi_1]$ lowest-lying excited singlet states, where $\text{M} = \text{Mg}, \text{Zn}, \text{Cd}, \text{Hg}$ and $\text{RG} = \text{Ne}, \text{Ar}, \text{Kr}, \text{Xe}$, have all been spectroscopically characterized except for the ZnNe and MgKr molecules [1–7]. It is important that the potential curves of all of these states be determined, both for our general understanding of bonding trends in van der Waals complexes as well as for use as ‘pair-potentials’ in modeling the interactions of metal atoms with more than one rare-gas atom, i.e., in

rare-gas clusters [8–11] and solid rare-gas matrices [9–12]. We report here a laser-induced fluorescence (LIF) study of the $\text{ZnNe}[^1\Pi_1 \leftarrow ^1\Sigma^+]$ transition, in which the bond lengths and the bond strengths of both the ground and upper states have been determined. Trends in bonding and in spectroscopic constants are discussed for all the analogous $\text{M} \cdot \text{RG}$ states.

2. Experimental

The apparatus has been described in detail elsewhere [3]. Briefly, Zn vapor in pure Ne gas (~ 9 atm pressure) was expanded continuously from an oven through a nozzle of ~ 0.125 mm diameter into a vacuum chamber pumped by a Roots system, creating a free supersonic jet expansion. Frequency-doubled light (BBO crystal, Skytek) from an excimer-pumped dye laser was passed into the free jet (via a Pellin–Broca prism system which excluded the visi-

* Corresponding author. Fax: +1 801 581 8433; e-mail: breckenridge@chemistry.chem.utah.edu

¹ Permanent address: Department of Chemistry, National University of Ireland, Maynooth, County Kildare, Ireland. Visiting Associate Professor, 1998.

ble dye laser light from the apparatus) to excite $\text{ZnNe}(^1\Pi_1, v') \leftarrow \text{ZnNe}(^1\Sigma^+, v'' = 0)$ transitions. Fluorescence from the $\text{ZnNe}(^1\Pi_1, v')$ states was detected at right angles to both the axis of the expansion and the excitation beam, through a UV band-pass filter ($\lambda_{\text{max}} = 2180 \text{ \AA}$, FWHM 230 \AA), with an Electron-Tubes 9816QB photomultiplier tube operated at 2100 V. The signal from the photomultiplier tube, via a 50 \Omega termination, was detected with a LeCroy 9310 AM digital-storage oscilloscope over an effective time-interval of $\sim 50 \text{ ns}$ which included the laser-excitation pulse. (The fluorescence lifetime of the $\text{Zn}(4s4p\pi) \cdot \text{Ne}[^1\Pi_1]$ state is $\sim 2 \text{ ns}$, much shorter than the 15 ns duration of the laser-excitation pulse.) The dye used in the dye laser was Stilbene 420 from Exciton.

3. Results

Shown in Fig. 1 is a laser-induced fluorescence (LIF) spectrum of three bands assigned as $\text{ZnNe}(^1\Pi_1, v') \leftarrow \text{ZnNe}(^1\Sigma^+, v'' = 0)$ transitions. There is a strong $\text{Zn}(4s4p^1P_1 \leftarrow 4s^2^1S_0)$ atomic transition,

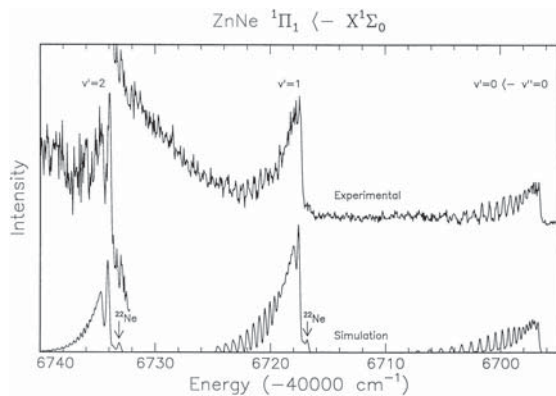


Fig. 1. Top: Experimental LIF spectrum of the $\text{Zn}(4s4p\pi) \cdot \text{Ne}[^1\Pi_1, v', J'] \leftarrow \text{Zn}(4s^2) \cdot \text{Ne}[^1\Sigma^+, v'' = 0, J'']$ transitions. Bottom: Computer simulations of these transitions, using the spectroscopic constants in Table 1 (values in brackets were used for the ground state), and assuming Morse function potential curves. All ZnNe isotopomers are included in their natural abundance percentages. (Boltzmann temperature, 6.5 K; laser line-width, 0.16 cm^{-1} ; relative intensities in the simulations of the three vibrational bands in this figure were calculated from Franck–Condon factors, using the spectroscopic constants in Table 1.)

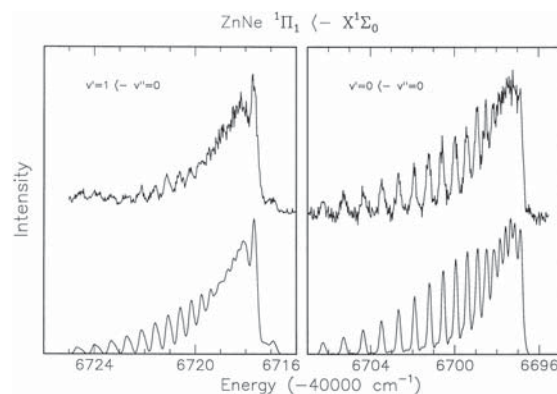


Fig. 2. Top: High-resolution LIF spectra of the (0,0) and (1,0) bands. Bottom: Computer simulations. (Boltzmann temperature, 6.5 K; laser line-width, 0.16 cm^{-1} .)

centered at 46745.4 cm^{-1} , due to the large amounts of Zn vapor present, the red wing of which is shown as the rising ‘baseline’ signal from ~ 46720 to $\sim 46740 \text{ cm}^{-1}$. The band at $\sim 46697 \text{ cm}^{-1}$ has been assigned as the (0,0) band, based on the following:

- (1) There is no sign of another band to the red at the expected progression frequency.
- (2) Computer simulations of the rotational structure of the three bands, including the expected isotopic shifts for all the ZnNe isotopomers, were consistent with the assignment of the band at $\sim 46697 \text{ cm}^{-1}$ as the (0,0) band.

The three bands in Fig. 1 were computer simulated assuming $\text{ZnNe}(^1\Pi_1, v', J') \leftarrow \text{ZnNe}(^1\Sigma^+, v'' = 0, J'')$ transitions. The line-strengths used for the rotational transitions were those appropriate for saturated transitions. Simulations with normal Hönl–London factors were less successful in reproducing the relative intensities, especially for the P-heads of the more intense (2,0) and (1,0) bands, and it appears that the transitions were partially saturated. A laser line-width of 0.16 cm^{-1} and a Boltzmann distribution of J'' levels with a temperature of 6.5 K were used in the simulations. Note that the reproducible isotopic structure to the red due to the Zn^{22}Ne isotopomers (9.2%) is clearly consistent with the assignment of the (1,0) and (2,0) bands. In Fig. 2, high-resolution experimental LIF spectra of the (0,0) and (1,0) bands are shown along with computer simulations of their rotational structure.

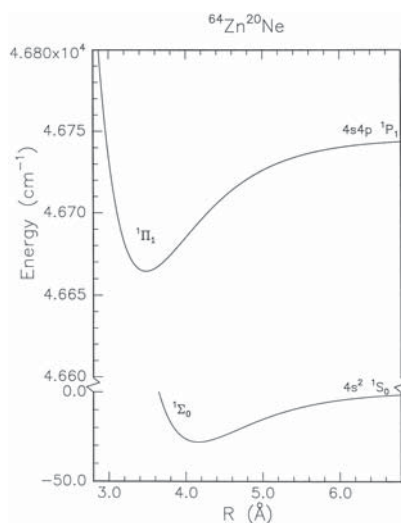


Fig. 3. Potential curves of the $\text{Zn}(4s^2) \cdot \text{Ne}(^1\Sigma^+)$ and $\text{Zn}(4s4p\pi) \cdot \text{Ne}(^1\Pi_1)$ states ($D_e'' = 27 \text{ cm}^{-1}$, $D_e' = 81 \text{ cm}^{-1}$).

Spectroscopic constants for the upper and lower states derived from the simulations are shown in Table 1. No hot bands were observed (even though $v'' = 1, 2$ levels should exist), and $\omega_e'' = 15 \pm 3 \text{ cm}^{-1}$ was estimated from ground-state ω_e values for the analogous MgNe, CdNe, and HgNe ground states (see Table 2). Shown in Fig. 3 are the Morse potential curves determined for the $\text{Zn}(4s^2)\text{Ne}(^1\Sigma^+)$ and

$\text{Zn}(4s4p\pi)\text{Ne}(^1\Pi_1)$ states. An ab initio calculation of the $\text{Zn}(4s^2)\text{Ne}(^1\Sigma^+)$ state has yielded $D_e' = 15 \text{ cm}^{-1}$; $R_e'' = 4.4 \text{ \AA}$ [13]. Such calculations are difficult, and routinely underestimate D_e values and overestimate R_e values [1,14–16], so the ab initio results [13] are quite consistent with our experimentally derived values of D_e'' and R_e'' .

In the analogous CdNe and HgNe molecules, where the $^1\Sigma^+$ ground-state D_0' values are accurately known ($\pm 2 \text{ cm}^{-1}$) from direct determinations of the dissociation limits of weakly-bound excited triplet states [1], Birge–Sponer extrapolation of the $^1\Pi \leftarrow ^1\Sigma^+$ vibrational progressions in those cases underestimate the true D_0' value of the $^1\Sigma^+$ state (and the D_0' value of the $^1\Pi_1$ state, of course), by ~ 11 and $\sim 8 \text{ cm}^{-1}$, respectively. We thus believe our derived D_0'' and D_0' values may be as much as 10 cm^{-1} too low. Also, the $\omega_e x_e'$ value for the $\text{ZnNe}(^1\Pi_1)$ state is based on only three bands, and may be uncertain to $\pm 0.2 \text{ cm}^{-1}$, yielding an experimental uncertainty in D_0' of $\pm 3 \text{ cm}^{-1}$. We therefore quote D_e'' and D_e' for the ZnNe states with the reasonable error limits of $+12$ and -3 cm^{-1} , respectively. Based on the CdNe and HgNe cases, we estimate that the true D_e' and D_e'' values for the ZnNe states are probably ~ 81 and $\sim 27 \text{ cm}^{-1}$, respectively.

Table 1
Spectroscopic constants for $^{64}\text{Zn}^{20}\text{Ne}$ states (all units in cm^{-1} except R_0 , R_e , which are in \AA)

	$\text{Zn}(4s^2) \cdot \text{Ne}(^1\Sigma^+)$	$\text{Zn}(4s4p\pi) \cdot \text{Ne}(^1\Pi_1)$	Transitions
D_0	$[20]^f, 10.3 \pm_{-3}^{12a}$	$[69]^f, 58.8 \pm_{-3}^{12b}$	–
D_e	$[27]^f, 18 \pm_{-3}^{12a,c}$	$[81]^f, 71.1 \pm_{-3}^{12b}$	–
ω_e	$[15 \pm 3]^c$	25.8 ± 0.4	–
$\omega_e x_e$	$[2.1]^e$	2.34 ± 0.2	–
B_0	0.0602 ± 0.0030	0.0873 ± 0.0030	$\Delta B_0 = 0.0271 \pm 0.0005$
B_e	$(0.0640 \pm 0.0030)^e$	0.0914 ± 0.0030	–
α_e	–	9.1×10^{-3d}	–
R_0	4.29 ± 0.10	3.56 ± 0.06	$\Delta R_0 = 0.73 \pm 0.02$
R_e	$(4.16 \pm 0.10)^e$	3.48 ± 0.06	–
$\nu_{0,0}$	–	–	46 696.9
$\nu_{1,0}$	–	–	46 718.0
$\nu_{2,0}$	–	–	46 734.4

^aFrom D_0' of $^1\Pi_1$ state, and a thermochemical cycle.

^bFrom a Birge–Sponer extrapolation.

^c ω_e value estimated from values of analogous MgAr, CdAr, HgAr states (see Table 2).

^dDerived from B_0' and B_1' only.

^eEstimated from Morse potential assuming $D_e'' = 27 \text{ cm}^{-1}$.

^fOur ‘best estimate’ (see text).

^gIf $D_e'' = 27 \text{ cm}^{-1}$, $\omega_e'' = 15 \text{ cm}^{-1}$, then $\omega_e x_e'' = \omega_e''^2 / 4D_e'' = 2.1 \text{ cm}^{-1}$ (Morse potential).

Table 2
Spectroscopic constants D_e , ω_e , R_e for M · RG states (D_e , ω_e values in cm^{-1} ; R_e values in ångström; estimated values in brackets)

State of atom M	M · Ne			M · Ar			M · Kr			M · Xe			
	Molecular electronic state	D_e	ω_e	R_e	D_e	ω_e	R_e	D_e	ω_e	R_e	D_e	ω_e	R_e
Mg ($3s^2S_0$)	$1\Sigma^+$	23 ± 5^e	14.0 ± 0.5^e	4.40 ± 0.15^e $R_0 = 4.67 \pm 0.15^e$	$[65 \pm 30]^{h,k}$	24.1 ± 1.0^h	4.49 ± 0.10^h	–	–	–	94 ± 80^c	–	4.56 ± 0.15^c
Zn ($4s^2S_0$)	$1\Sigma^+$	$[27]^{d,k}$	15 ± 3^d	$\sim 4.16^d$	$[85 \pm 30]^{c,k}$	22 ± 3^f	4.18 ± 0.07^c	$[110 \pm 40]^{c,k}$	$[13.5]^e$	4.20 ± 0.10^c	162 ± 2^i	13 ± 2^i	$[4.4]^{a,i}$
Cd ($5s^2S_0$)	$1\Sigma^+$	$18_{-3}^{1,2d}$	13 ± 1^g	$(R_0 = 4.29 \pm 0.10)^d$	107 ± 2^c	19 ± 1^g	4.31 ± 0.06^c	130 ± 2^c	17 ± 1^g	–	183 ± 2^c	–	a
Hg ($6s^2S_0$)	$1\Sigma^+$	46 ± 2^e	18.5 ± 1.0^j	3.90 ± 0.02^c	142 ± 2^c	23.5 ± 1.0^j	3.99 ± 0.01^c	178 ± 2^c	20 ± 1^j	$[4.07]^{b,c}$	254 ± 2^c	18 ± 1^j	$[4.25]^{b,c}$
Mg ($3s3p^1P_1$)	1Π	53 ± 6^e	21.1 ± 1.2^e	$[3.9]^f$	368 ± 30^h	43 ± 1^h	3.27 ± 0.05^h	–	–	–	1500 ± 80^c	97.5 ± 1.0^c	3.07 ± 0.10^c
Zn ($4s4p^1P_1$)	1Π	$[81]^{d,k}$	25.8 ± 0.4^d	3.48 ± 0.06^d	706 ± 40^c	62 ± 1^c	2.97 ± 0.03^c	1466 ± 50^c	81 ± 1^c	2.79 ± 0.03^c	3341 ± 100^i	117 ± 2^i	$[2.8]^{a,i}$
Cd ($5s5p^1P_1$)	1Π	$71_{-3}^{1,2d}$	23.5 ± 1.0^c	3.61 ± 0.06^c	544 ± 10^c	48 ± 1^c	3.28 ± 0.03^c	1036 ± 40^c	57 ± 1^c	–	a	a	a
Hg ($6s6p^1P_1$)	1Π	97 ± 2^e	27 ± 1^c	3.41 ± 0.02^c	542 ± 10^c	50.3 ± 0.2^c	3.28 ± 0.08^c	1495 ± 40^c	69.1 ± 1.0^c	$[2.93]^{b,c}$	$3595 \pm 800^{c,j}$	$99 \pm 10^{c,j}$	$[2.95 \pm 0.15]^{b,j}$

^a Excited state predissociates rapidly.

^b 'Kong's rule' estimate of ground-state R_e values; excited state estimates by Franck–Condon simulations, given the ground-state estimates.

^c Ref. [1].

^d This Letter.

^e Ref. [2].

^f Ref. [3].

^g Ref. [4].

^h Ref. [5].

ⁱ Ref. [6].

^j Ref. [7]; only 3 bands at very high ν' were observed, so we believe the $1\Pi_1$ state spectroscopic values are quite uncertain.

^k Our 'best estimate'.

4. Discussion

As can be ascertained from Table 2, the ZnNe molecule follows a general trend for the M·RG states. The ground $^1\Sigma^+$ state of Zn·Ne is quite weakly bound, $D_e'' \approx 27 \text{ cm}^{-1}$, with a large bond distance, $R_e'' \approx 4.16 \text{ \AA}$, while the Zn(4s4p π)·Ne($^1\Pi_1$) excited state is much more strongly bound, $D_e' = 81 \text{ cm}^{-1}$, and has a shorter bond length, $R_e' = 3.48 \pm 0.06 \text{ \AA}$. As the Ne atom approaches the Zn(4s 2) filled sub-shell, the small dispersive attraction at large R is soon overcome by Zn(4s 2)/Ne(2p σ) 2 exchange repulsion, resulting in a weak $^1\Sigma^+$ ground-state van der Waals bond. In contrast, in the $^1\Pi_1$ excited state, the Ne approaches the highest-energy Zn(4p π) electron along its nodal axis [1], with little initial repulsion. At large R , in addition to Zn(4p π)/Ne(2p π) and Zn(4s)/Ne(2p σ) dispersive attraction, there is an attractive interaction with the large, perpendicular quadrupole moment of the Zn(4s4p π) state (quadrupole/induced-dipole being the longest range term). At shorter distances, where R is comparable to or smaller than the 'size' of the quite diffuse excited Zn(4p π) orbital, the Ne atom begins to experience an attractive 'ion/induced-dipole' type force which would approach that of the Zn(4s $^+$)/Ne ground-state ion if there were no Zn(4p π)/Ne(2p π) repulsion.

As seen in Table 2, the M·RG bond energies (both ground- and excited-state) increase in the order Ne < Ar < Kr < Xe for a given M, because all of the attractive forces increase with the polarizability of the RG atom (in \AA^3) [17]: Ne, 0.396; Ar, 1.64; Kr, 2.48; and Xe, 4.04. There is a particularly large increase from Ne to Ar, since there is a four-fold increase in polarizability. On the other hand, the effective 'hard-sphere' radii (in \AA) [18] of the RG atoms do not increase so rapidly: Ne, ~ 1.4 ; Ar, ~ 1.7 ; Kr, ~ 1.8 ; Xe, ~ 2.0 , so the increase in attractive forces with polarizability of the RG atom is greater than the increase in the repulsive forces at intermediate distances R , and the bond strengths thus increase in the order Ne < Ar < Kr < Xe. This is especially obvious for the more strongly-bound $^1\Pi_1$ states, where despite the increase in RG atom 'size' the bond lengths (when known) actually *decrease* substantially in the order Ne > Ar > Kr, as the bond strengths increase rapidly in the same order.

These same kinds of trends are observed for the D_e and R_e values of the analogous ground-state M(ns) $^+$ /RG ions. For example, for the Mg(3s) $^+$ /RG states, where RG = Ne, Ar, Kr, the D_e values increase substantially (200, 1290, 1949 cm^{-1} , respectively [15,16,19]) while the R_e values decrease slightly (~ 3.15 , 2.80, $\sim 2.8 \text{ \AA}$, respectively [19–21]).

Acknowledgements

We are grateful to the National Science Foundation for financial support of this work. We thankfully acknowledge the use of the computer facilities provided by the Center for High Performance Computing at the University of Utah. The SP has been partially funded by NSF grant No. CDA 9601580 and a Shared University Research (SUR) grant from IBM.

References

- [1] W.H. Breckenridge, C. Jouviet, B. Soep, in: M. Duncan (Ed.), *Advances in Metal and Semiconductor Clusters*, vol. 3, JIA Press, Greenwich, CT, 1995.
- [2] I. Wallace, W.H. Breckenridge, *J. Chem. Phys.* 98 (1993) 2768.
- [3] I. Wallace, R.R. Bennett, W.H. Breckenridge, *Chem. Phys. Lett.* 153 (1988) 127.
- [4] D.J. Funk, A. Kvaran, W.H. Breckenridge, *J. Chem. Phys.* 90 (1989) 2915.
- [5] R.R. Bennett, J.G. McCaffrey, I. Wallace, D.J. Funk, A. Kowalski, W.H. Breckenridge, *J. Chem. Phys.* 90 (1989) 2139.
- [6] I. Wallace, J. Kaup, W.H. Breckenridge, *J. Phys. Chem.* 95 (1991) 8060.
- [7] T. Tsuchizawa, K. Yamanouchi, S. Tsuchiya, *J. Chem. Phys.* 89 (1988) 4646.
- [8] J.G. Kaup, W.H. Breckenridge, *J. Phys. Chem.* 99 (1995) 13701.
- [9] J.G. McCaffrey, P.N. Kerins, *J. Chem. Phys.* 106 (1997) 7885.
- [10] P.N. Kerins, J.G. McCaffrey, *J. Chem. Phys.* 109 (1998) 3131.
- [11] W.H. Breckenridge, M.D. Morse, J.G. McCaffrey, *J. Chem. Phys.* 109 (1998) 3139.
- [12] V.A. Bracken, P.N. Kerins, P. Gürtler, J.G. McCaffrey, *J. Chem. Phys.* 107 (1997) 5300.
- [13] A.W.K. Leung, W.H. Breckenridge (to be published).

- [14] A.W.K. Leung, R.R. Julian, W.H. Breckenridge (submitted).
- [15] S. Massick, W.H. Breckenridge, *Chem. Phys. Lett.* 257 (1996) 465.
- [16] J.G. Kaup, W.H. Breckenridge, *J. Chem. Phys.* 107 (1997) 2180.
- [17] E.A. Mason, E.W. McDaniel, *Transport Properties in Gases*, Wiley, New York, 1988.
- [18] J.O. Hirschfelder, C.F. Curtiss, R.B. Bird, *Molecular Theory of Gases and Liquids*, Wiley, New York, 1954.
- [19] J.E. Reddic, M.A. Duncan (submitted).
- [20] C.T. Spurlock, J.S. Pilgrim, M.A. Duncan, *J. Chem. Phys.* 105 (1996) 7876.
- [21] R.R. Julian, A.W.K. Leung, D. Bellert, W.H. Breckenridge (to be submitted).